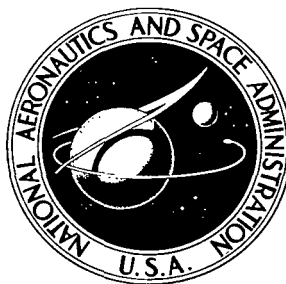


NASA TECHNICAL NOTE



NASA TN D-5292

C. 1

NASA TN D-5292



LOAN COPY: RETURN TO
AFWL (WLIL-2)
KIRTLAND AFB, N MEX

METHOD FOR PREDICTION OF
PUMP CAVITATION PERFORMANCE FOR
VARIOUS LIQUIDS, LIQUID TEMPERATURES,
AND ROTATIVE SPEEDS

by Robert S. Ruggeri and Royce D. Moore

*Lewis Research Center
Cleveland, Ohio*



METHOD FOR PREDICTION OF PUMP CAVITATION PERFORMANCE FOR
VARIOUS LIQUIDS, LIQUID TEMPERATURES, AND ROTATIVE SPEEDS

By Robert S. Ruggeri and Royce D. Moore

Lewis Research Center
Cleveland, Ohio

NATIONAL AERONAUTICS AND SPACE ADMINISTRATION

For sale by the Clearinghouse for Federal Scientific and Technical Information
Springfield, Virginia 22151 - CFSTI price \$3.00

ABSTRACT

A method for predicting the cavitation performance of pumps with various liquids, liquid temperatures, and rotative speeds is presented. Both theoretical and experimental studies used in formulating the method are discussed. Good agreement was obtained in comparisons between experimental and predicted results of cavitation performance for several pumps operated in liquids that exhibit a wide range of physical properties. Use of the method requires that two sets of test data be available for the pump and operating conditions of interest, but these data need not be for the same liquid, temperature, or pump speed. Numerical examples are presented.

METHOD FOR PREDICTION OF PUMP CAVITATION PERFORMANCE FOR VARIOUS LIQUIDS, LIQUID TEMPERATURES, AND ROTATIVE SPEEDS

by Robert S. Ruggeri and Royce D. Moore

Lewis Research Center

SUMMARY

A method that predicts the cavitation performance for pumps and inducers is presented. The present study shows that the method consistently provided good agreement between experimental and predicted performance for an inducer and five different pumps operated with a variety of liquids that have widely diverse physical properties. Use of the method requires that two sets of appropriate test data be available for each pump and operating condition of interest. These test data need not necessarily be for the same liquid, liquid temperature, or rotative speed. At least one set of data, however, must provide measurable thermodynamic effects of cavitation. From these reference tests, accurate predictions of cavitation performance for a given pump can be made for other liquids, liquid temperatures, and/or rotative speeds. Predictions are made on the basis of flow similarity with cavitation and, thus, predicted values apply to the same conditions of flow coefficient and pump cavitation performance level used in obtaining the reference test data.

INTRODUCTION

Cavitation, which is the formation and collapse of vaporous cavities in flowing liquids, can degrade the performance of pumps and other hydraulic equipment. Because cavitation is a vaporization process that involves heat and mass transfer, the physical properties of the liquid and its vapor and the flow conditions can affect the cavitation process and thus the cavitation performance of hydraulic equipment as well. The combined effects of fluid properties, flow conditions, and heat transfer, termed thermodynamic effects of cavitation, can improve cavitation performance. For example, cavitation studies with pumps and venturis (refs. 1 to 10) have shown that, for certain liquids and/or liquid temperatures, the net positive suction head (NPSH) requirements can be signifi-

cantly less than that obtained for room-temperature water. (NPSH is defined as the total pressure above vapor pressure at the inlet to a pump.) This improvement (decrease) in inlet pressure requirements is attributed to the varying degrees of evaporative cooling associated with the cavitation process. Because of the evaporative cooling, the cavity pressure and the vapor pressure of the liquid adjacent to the cavity are decreased relative to the vapor pressure of the bulk liquid. This decrease in cavity pressure retards the rate of further vapor formation, thereby allowing the pump to operate at lower values of NPSH than would otherwise be possible. The NPSH requirement for a pump operating at a given head rise and flow condition is reduced by the amount corresponding to the decrease in cavity pressure. The accurate prediction of thermodynamic effects of cavitation is therefore essential to an optimum flow system that is designed to operate with cavitation.

Various analyses that relate thermodynamic effects of cavitation to pump performance have been proposed (refs. 1 to 7). Although these studies are useful in predicting trends, their applicability is somewhat limited because either (1) the analysis does not predict quantitative values or (2) the experimental data used did not adequately cover the range of fluid properties and flow conditions of current interest, particularly in the aerospace field. Also, existing analyses do not account for effects of heat transfer, flow velocity (and its relation to heat transfer), or pump scale.

Subsequent to the studies of references 1 to 7, several investigations have been conducted to study in detail the thermodynamic effects of cavitation and its relation to the cavitation performance of various flow devices such as venturis, pumps, and pump inducers (refs. 9 to 12). From venturi studies, a method for predicting thermodynamic effects of cavitation as a function of the liquid used, liquid temperature, flow velocity, and body scale for a given venturi design was formulated in references 10 and 11. Use of the method requires reference data obtained by experiment. The method, based primarily on Freon-114 cavitation results, was later demonstrated to be applicable to the prediction of cavitation performance for pumps and inducers (refs. 9, 13, and 14). The applicability of the method was extended over a wide range of fluid properties and flow conditions by conducting a subsequent cavitation study using liquid hydrogen (ref. 15) in a venturi of identical design to that previously used. These hydrogen data were then used in conjunction with other available cavitation data for the same venturi design to re-evaluate the exponents of the prediction equation. The new exponents, which are now based on a wider range of variables, are reported in reference 16. The resulting slight changes have little effect on predicted results of references 9, 13, and 14.

The objective of this study was to present, in a comprehensive and detailed manner, a method for the prediction of cavitation performance for pumps and inducers. The method presented is based on, and is an extension of, the method already reported in reference 16 for venturis. It is applicable to various liquids, liquid temperatures, and pump rotative speeds. A prerequisite to this prediction method is that similarity of the cavitating flow over the suction surface of the blade be maintained for all conditions to

which the method is applied. Use of the method requires that two sets of appropriate test data be available for each pump and operating condition of interest.

Cavitation performance data for several research and commercial pumps, obtained with a variety of liquids over a range of conditions, are compared with predicted results using the derived method. Selective data for an inducer and two centrifugal pump impellers operated with liquid hydrogen are presented and compared with predictions to show magnitude changes in thermodynamic effects of cavitation with hydrogen temperature, pump speed, flow coefficient, and geometric design. A discussion on the implementation of the method, including numerical examples, is also presented.

ANALYSIS

Development of Basic Relations

Cavitation similarity parameters. - The conventional cavitation parameter for dynamic similarity of cavity flow is of the form

$$K \equiv \frac{h_0 - h_v}{\frac{V_0^2}{2g}} \quad (1)$$

where free-stream static-pressure head h_0 and free-stream velocity V_0 are those required to produce a given amount of cavitation, and h_v is the vapor pressure head corresponding to free-stream temperature. (Symbols are defined in appendix A.) Equation (1) is based on the assumption that the cavity surface is at a constant pressure equal to free-stream vapor pressure. However, because of the thermodynamic effect of cavitation, cavity pressure can be significantly less than free-stream vapor pressure. In the case of liquid hydrogen, cavity pressures can be less than free-stream vapor pressure by several hundred feet of liquid (refs. 15 and 16). Thus, a more general cavitation parameter is one in which h_v in equation (1) is replaced by the actual cavity pressure h_c . However, venturi cavitation studies have shown that, within a given fixed cavity, the pressure varies with axial distance (refs. 10, 12, and 16), and thus it becomes necessary to specify a particular reference cavity pressure. Herein, as in references 10, 11, and 16, the minimum cavity pressure head $h_{c, \min}$, which occurs near the cavity leading edge, is used to define a modified cavitation parameter for developed cavities; namely,

$$K_{c, \min} = \frac{h_0 - h_{c, \min}}{\frac{V_0^2}{2g}} = K + \frac{h_v - h_{c, \min}}{\frac{V_0^2}{2g}} = K + \frac{\Delta h_v}{\frac{V_0^2}{2g}} \quad (2)$$

In the absence of thermodynamic effects of cavitation, cavity pressure corresponds to free-stream vapor pressure ($\Delta h_v = 0$) and thus $K_{c, \min} = K$. The usefulness of $K_{c, \min}$ as a similarity parameter has been demonstrated by the studies of references 10 and 16 wherein it was shown that, for fixed-size cavities in a given venturi design ($\Delta X/D = \text{Constant}$), the modified parameter $K_{c, \min}$ remained essentially constant for different liquids, liquid temperatures, flow velocities, and venturi scales, whereas the corresponding K values, which are based on stream vapor pressure, varied widely. For constant values of $K_{c, \min}$ and V_0 in equation (2), a change in the minimum cavity pressure $h_{c, \min}$ (maximum depression) results in an equal change in stream static pressure under conditions of flow similarity. As discussed later in this section, this direct correspondence between $h_{c, \min}$ and h_0 provides the basis for use of equation (2) in the prediction of cavitation performance (free-stream static-pressure requirements) for devices such as pumps and inducers.

The magnitude of cavity pressure depression is a complex function of body geometry, flow velocity, and the heat- and mass-transfer processes involved, as well as the physical properties of the liquid and its vapor. Because of the complexity of the cavitation process, the value of $h_{c, \min}$ or Δh_v is not generally known or predictable for any arbitrary flow device, liquid, and/or flow situation. However, performance predictions for a given flow device can be made indirectly by experimentally determining a reference value of Δh_v and, thus, $K_{c, \min}$ by using practically any convenient combination of test liquid, liquid temperature, or flow velocity that yields a measurable Δh_v . Then by use of the method detailed in references 10, 11, 16, and herein, predicted values of Δh_v , relative to the reference test value, are calculated for other liquids, liquid temperatures, and/or flow velocities of interest. With the experimentally determined value of $K_{c, \min}$, which remains constant for geometrically similar cavities, the free-stream static-pressure requirement h_0 is predicted by use of equation (2).

Geometric similarity of the cavitated region is essential to the use of $K_{c, \min}$ for prediction purposes. In a given pump or inducer, cavitation performance is of course dependent on the vapor cavity volume present within the blade passages, although the presence of small vapor cavities on the suction surface of the blade will not necessarily affect the performance. It is reasonable to assume that, for operation of a pump at a constant flow coefficient (similarity of entering flow), the cavity on the suction surface of the blade, and thus the vapor volume corresponding to a specified head-rise coefficient ratio ψ/ψ_{NC} , is essentially constant irrespective of the liquid, liquid temperature, and/or rotative speed. This criterion of fixed-vapor cavity volume, together with the

previously discussed constancy of $K_{c, \min}$, allows the prediction method developed for venturis to be extended to pumps and inducers. The prediction method, as applied to pumps, is described in the following section.

Similarity relations for pumps. - Pump cavitation performance is generally presented in terms of the net positive suction head (NPSH) required at a specified ratio of the head-rise coefficient with cavitation to that without cavitation (ψ/ψ_{NC}). The NPSH is defined as the margin of fluid total head above fluid vapor pressure head at the pump inlet; or in terms of inlet static-pressure head and velocity head,

$$\text{NPSH} = h_0 + \frac{V_1^2}{2g} - h_v$$

In terms of net positive suction head, equation (2) may be written as

$$\frac{V_1^2}{2g} (K_{c, \min} + 1.0) = h_0 + \frac{V_1^2}{2g} - h_v + \Delta h_v$$

or

$$K_{c, \min} = \frac{\text{NPSH} + \Delta h_v}{\frac{V_1^2}{2g}} - 1.0 \quad (3)$$

where V_1 in the preceding equations is analogous to V_0 for venturis. Because the value of $K_{c, \min}$ is constant for geometrically similar cavities in a given flow device, it follows (from eq. (3)) that

$$\frac{\text{NPSH}_{\text{ref}} + (\Delta h_v)_{\text{ref}}}{\text{NPSH} + \Delta h_v} = \left[\frac{(V_1)_{\text{ref}}}{V_1} \right]^2 \quad (4)$$

where the subscript ref denotes a reference value that must be established by experiment. With flow similarity, the fluid velocity at the pump inlet is proportional to pump rotative speed N , and thus equation (4) may be expressed as

$$\frac{\text{NPSH}_{\text{ref}} + (\Delta h_v)_{\text{ref}}}{\text{NPSH} + \Delta h_v} = \left(\frac{N_{\text{ref}}}{N} \right)^2 \quad (5)$$

Equation (5) may be used to predict the required NPSH for a particular pump operated with cavitation at a fixed flow coefficient and head coefficient ratio but with changes in liquid, liquid temperature, and/or rotative speed. For a fixed rotative speed, equation (5) reduces to

$$\text{NPSH}_{\text{ref}} - \text{NPSH} = \Delta h_v - (\Delta h_v)_{\text{ref}} \quad (6)$$

which states that a change in NPSH requirements for different liquids and/or liquid temperatures is equal to the change in the maximum pressure depression Δh_v within the cavitated region.

The procedure for estimating Δh_v , required for use in equations (5) and (6), is discussed in the following section.

Determination of Cavity Pressure Depressions

Thermodynamic effects of cavitation. - A method for estimating values of Δh_v for untested liquids and conditions from known reference values was previously reported for venturis in references 10, 11, and 16. However, the pertinent results that lead to the development of the prediction method for pumps presented herein are included for convenience and clarity.

The previously mentioned reduction in pressure (below free-stream vapor pressure) within cavitated regions of various liquids is attributed to evaporative cooling of a thin layer of liquid adjacent to the cavity. This cooling causes a decrease in the vapor pressure of the affected liquid layer and a corresponding decrease in cavity pressure provided that the liquid and its vapor are locally in thermodynamic equilibrium and no permanent gases are present.

Heat balance. - The magnitude of cavity pressure depression can be estimated by setting up (as an initial step) a heat balance between the heat required for vaporization and the heat drawn from the liquid surrounding the cavity; that is,

$$\rho_v \mathcal{V}_v L = \rho_l \mathcal{V}_l C_l (\Delta T) \quad (7)$$

where \mathcal{V}_l represents the volume of the thin layer of liquid that is cooled during vaporization. The cooled layer of liquid is only a fraction of the total liquid flow. For small changes in temperature of the liquid layer, the temperature drop ΔT may be expressed as

$$\Delta T = \Delta h_v \left(\frac{1}{\frac{dh_v}{dT}} \right)$$

where dh_v/dT is the slope of the vapor pressure-temperature curve. With the use of this relation equation (7) becomes

$$\Delta h_v = \frac{\rho_v \gamma_v L}{\rho_l \gamma_l C_l} \left(\frac{dh_v}{dT} \right) \quad (8)$$

An accurate solution of equation (8), which accounts for changes in fluid properties as the equilibrium temperature drops because of vaporization, is presented in reference 10. Values of Δh_v as a function of the vapor- to liquid-volume ratio based on the solution of reference 10 are presented in figure 1 for liquid hydrogen, water, butane, and

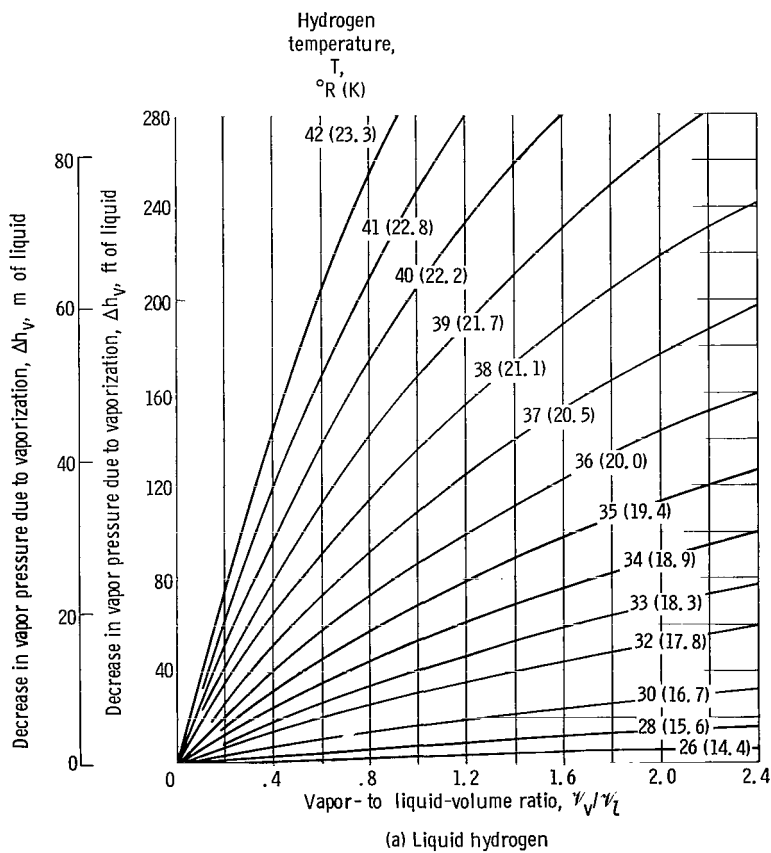
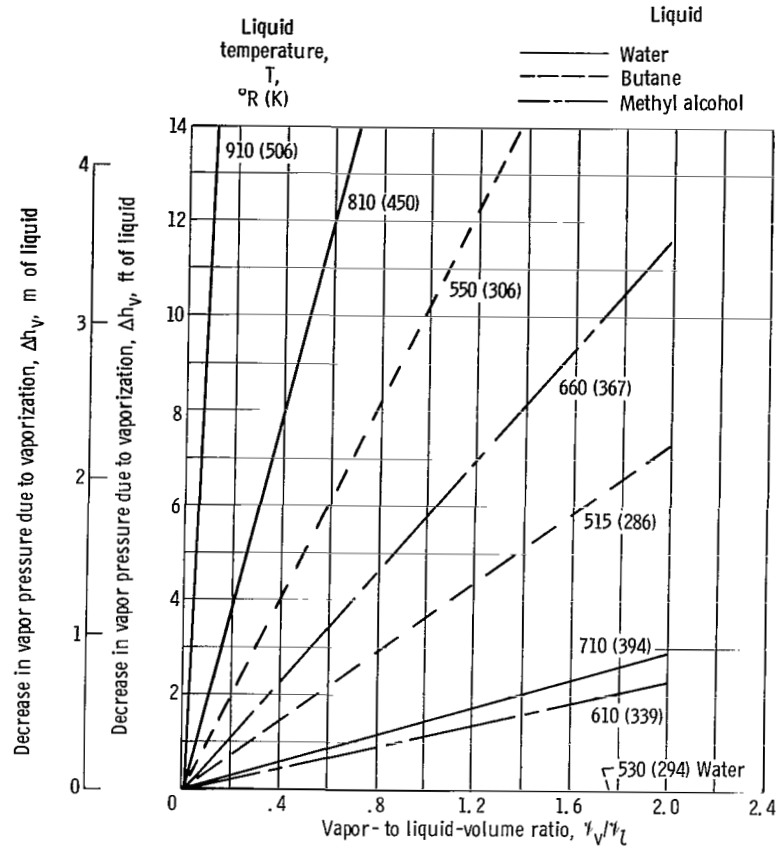


Figure 1. - Vapor pressure depression as function of vapor- to liquid-volume ratio for various liquids and liquid temperatures.



(b) Water, butane, and methyl alcohol.

Figure 1. - Concluded.

methyl alcohol at various temperatures. For a given value of γ_v/γ_l , the depression in cavity pressure can vary by several orders of magnitude depending on liquid and liquid temperature.

An approximate solution of equation (8) is obtained through the use of the Clausius-Clapeyron equation to approximate the slope of the vapor pressure-temperature curve. The Clausius-Clapeyron equation states that

$$\frac{\Delta h_v}{\Delta T} = \frac{J}{\rho_l} \frac{L}{T(\nu_v - \nu_l)} \frac{g_c}{g} \quad (9)$$

where ν_v and ν_l are the specific volume of the vapor and liquid, respectively. Except near the critical temperature, $\nu_l \ll \nu_v$ and thus ν_l can be neglected. Setting $\nu_l = 0$ and substituting for $\Delta h_v/\Delta T$ (eq. (9)) in equation (8) gives

$$\Delta h_v \cong J \left(\frac{\rho_v}{\rho_l} \right)^2 \left(\frac{L^2}{C_l T} \right) \left(\frac{\gamma_v}{\gamma_l} \right) \left(\frac{g_c}{g} \right) \quad (10)$$

This expression provides a useful and close approximation of the curves presented in figure 1.

The vapor- to liquid-volume ratio γ_v/γ_l in any real flow situation is not known and cannot be measured directly, and thus the values of this ratio from figure 1 are used only in a relative sense. Useful predictions for geometrically similar cavities have been made by experimentally establishing an effective or reference value of γ_v/γ_l through the determination of cavity-pressure depressions Δh_v for one flow device, liquid, temperature, and velocity. Then values of γ_v/γ_l for other geometrically similar flow devices, liquids, liquid temperatures, and flow velocities are estimated relative to this reference value, as described subsequently. With these predicted values of γ_v/γ_l and figure 1, determination of Δh_v relative to reference data is possible.

Estimation of vapor- to liquid-volume ratio and cavity-pressure depression. - Theoretical analyses, coupled with experimental venturi cavitation results (refs. 10, 11, and 16), led to the development of the following expression relating the reference and predicted values of vapor- to liquid-volume ratio:

$$\left(\frac{\gamma_v}{\gamma_l} \right)_{\text{pred}} = \left(\frac{\gamma_v}{\gamma_l} \right)_{\text{ref}} \left(\frac{\alpha_{\text{ref}}}{\alpha} \right)^{1.0} \left(\frac{V_1}{V_{1,\text{ref}}} \right)^{0.8} \left(\frac{D}{D_{\text{ref}}} \right)^{0.2} \left[\frac{\left(\frac{\Delta X}{D} \right)}{\left(\frac{\Delta X}{D} \right)_{\text{ref}}} \right]^{0.3} \quad (11)$$

As previously discussed in the section Similarity relations for pumps, pump inlet velocity V_1 is proportional to pump rotative speed N under conditions of flow similarity. Also, for a given pump operated at a constant flow coefficient ϕ and a constant value of ψ/ψ_{NC} , cavity length (ΔX of eq. (11)) is considered to remain essentially constant for various liquids, liquid temperatures, and pump rotative speeds. Thus, when applied to a particular pump, equation (11) becomes

$$\left(\frac{\gamma_v}{\gamma_l} \right)_{\text{pred}} = \left(\frac{\gamma_v}{\gamma_l} \right)_{\text{ref}} \left(\frac{\alpha_{\text{ref}}}{\alpha} \right)^{1.0} \left(\frac{N}{N_{\text{ref}}} \right)^{0.8} \quad (12)$$

With $\left(\frac{\gamma_v}{\gamma_l} \right)_{\text{pred}}$ established, relative to the known reference value, the corresponding Δh_v value may be determined from either equation (10) or from the curves of

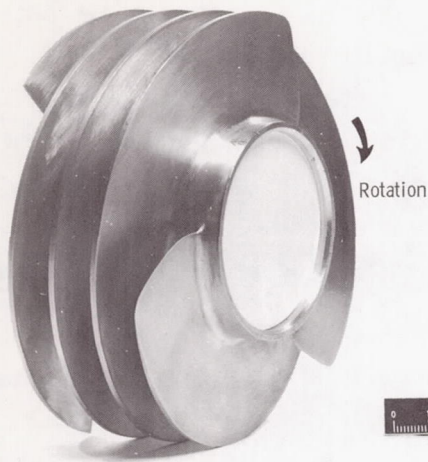
Δh_v against γ_v/γ_l similar to those of figure 1 for any liquid or liquid temperature of interest. With Δh_v known, the NPSH requirements may then be predicted by use of equation (5) (eq. (6) if $N = \text{constant}$). It should be emphasized that, because of the implied assumption of flow similarity used in this analysis, a predicted value of required NPSH applies only to the particular pump and the specific operating conditions of φ and ψ/ψ_{NC} used to obtain the required test data.

For pumps, the direct measurement of $(\Delta h_v)_{\text{ref}}$, needed for use in the prediction equations, is not feasible. However, an estimate of Δh_v is possible without measuring cavity pressure directly. For a particular pump, this estimation requires that two sets of experimental data be obtained to determine the NPSH requirement at each value of ψ/ψ_{NC} and flow coefficient φ of interest. These tests need not necessarily be for the same liquid, liquid temperature, or pump rotative speed; however, at least one of these must yield measurable thermodynamic effects of cavitation. Measured values of NPSH and rotative speed N from one of the two test conditions are arbitrarily chosen as the reference values in equation (5). Because both Δh_v and $(\Delta h_v)_{\text{ref}}$ are unknown, an iterative procedure is required for the solution of equation (5). First, a value of $(\Delta h_v)_{\text{ref}}$ is assumed. The corresponding $(\gamma_v/\gamma_l)_{\text{ref}}$ can be obtained from equation (10) (or equivalent curves of fig. 1). The predicted γ_v/γ_l for the second test condition is then calculated from equation (12), and the corresponding value of Δh_v is then obtained from equation (10) (or equivalent curves of fig. 1). Successive calculations are made until the values of Δh_v and $(\Delta h_v)_{\text{ref}}$ satisfy equation (5). With the value of $(\Delta h_v)_{\text{ref}}$ once determined, values of Δh_v and, consequently, the NPSH requirements can be predicted for other liquids, liquid temperatures, or pump rotative speeds by the use of equation (5). As indicated in the preceding paragraph, the predicted values apply only to a particular pump and specific values of ψ/ψ_{NC} used to obtain the necessary test data (i. e., values of ψ/ψ_{NC} and φ corresponding to $\Delta h_{v, \text{ref}}$).

Further details on the implementation of the prediction method are presented in appendix B. Numerical examples, which use test data obtained under various conditions, are included.

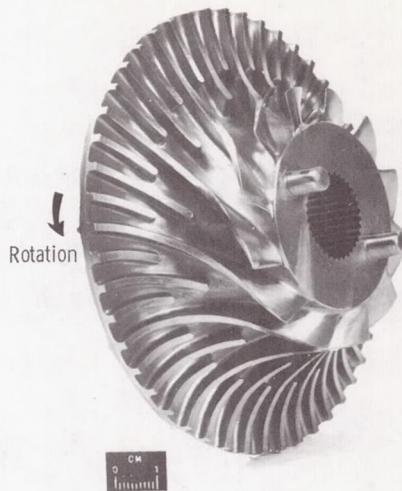
APPARATUS AND PROCEDURE

The test rotors used in the present study are shown in figure 2. Some of the geometric features of each rotor are also presented in the figure. The flat-plate helical inducer (fig. 2(a)) is the same as that described fully in reference 9. The centrifugal pump impeller with the 2.67-inch (6.78-cm) inlet blade tip diameter, herein termed impeller A (fig. 2(b)), is described in reference 17. The other centrifugal impeller (inlet blade tip



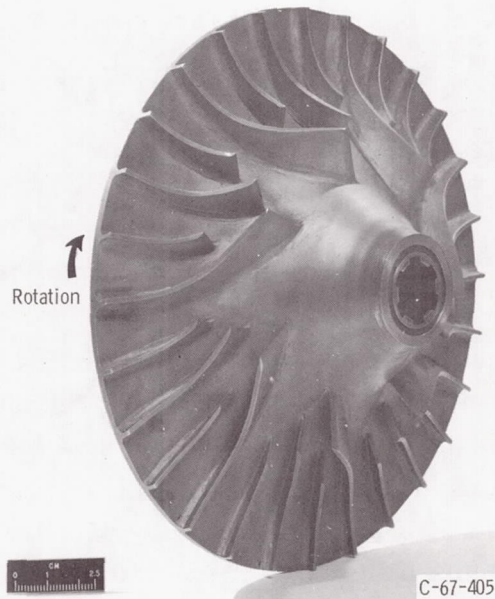
C-67-423

(a) Flat-plate helical inducer. Tip diameter, 4.986 inches (12.66 cm); hub diameter, 2.478 inches (6.29 cm); number of blades, 3; inlet tip blade angle, 84° (from axial direction).



C-67-1782

(b) Impeller A, centrifugal pump. Inlet blade tip diameter, 2.67 inches (6.78 cm); hub diameter at inlet, 1.87 inches (4.75 cm); overall diameter, 4.56 inches (11.58 cm); number of blades, 12; number of splitter vanes, 12 primary and 24 secondary; inlet tip blade angle, 71.3° (from axial direction).



C-67-405

(c) Impeller B, centrifugal pump. Inlet blade tip diameter, 3.86 inches (9.80 cm); hub diameter, 1.54 inches (3.91 cm); overall diameter, 7.44 inches (18.90 cm); number of blades, 7; number of splitter vanes, 7 primary and 14 secondary; inlet tip blade angle, 68° (from axial direction).

Figure 2. Test rotors.

diam, 3.86 in. or 9.80 cm), herein termed impeller B, is shown in figure 2(c) and is described in reference 18. The impellers used for this study were those for which sufficient data were available to check the prediction method. They do not necessarily represent the best designs for good cavitation performance. The rotors were tested in the liquid-hydrogen test facilities located at the NASA Plum Brook Station.

The test procedure used to obtain the data was the same for the three rotors. Throughout each test run, the liquid temperature, rotative speed, and flow coefficient were held constant. The NPSH was steadily reduced from a value corresponding to non-cavitating conditions ($\psi/\psi_{NC} = 1.0$) to a value that corresponds to about $\psi/\psi_{NC} = 0.7$. This same procedure was used for each liquid temperature, rotative speed, and flow coefficient studied.

RESULTS AND DISCUSSION

The prediction method was applied to an axial-flow inducer and several centrifugal pump impellers. These rotors were operated in several different liquids at various liquid temperatures. Experimental and predicted cavitation performance results are compared for (1) an inducer operated in liquid hydrogen at various temperatures, (2) two centrifugal pump impellers operated at various values of flow coefficient and rotative speed in constant-temperature hydrogen, and (3) several small commercial centrifugal pumps operated in a variety of liquids, each over a temperature range. Experimental data for the commercial pumps are taken from references 1 and 2.

Inducer Cavitation Performance

The cavitation performance for the 4.986-inch- (12.664-cm-) diameter research inducer shown in figure 2(a) is presented in figure 3. The data are for liquid hydrogen at temperatures from 27.5° to 36.6° R (15.3 to 20.3 K) and for constant values of flow coefficient and rotative speed. As expected, for a given value of the head-rise coefficient ratio ψ/ψ_{NC} , the required NPSH decreases rapidly with increasing hydrogen temperature. The performance results obtained at 27.5° and 31.7° R (15.3 and 17.6 K) were arbitrarily chosen as reference test data to predict the NPSH requirements for hydrogen at 34.3° and 36.6° R (19.1 and 20.3 K). The predicted NPSH requirements (dashed lines of fig. 3) agree with experimental results.

The magnitude of the thermodynamic effects of cavitation realized at the various temperatures for ψ/ψ_{NC} of 0.9 and 0.8 are listed in table I. For both values of ψ/ψ_{NC} , the Δh_v values increased rapidly with increasing temperature.

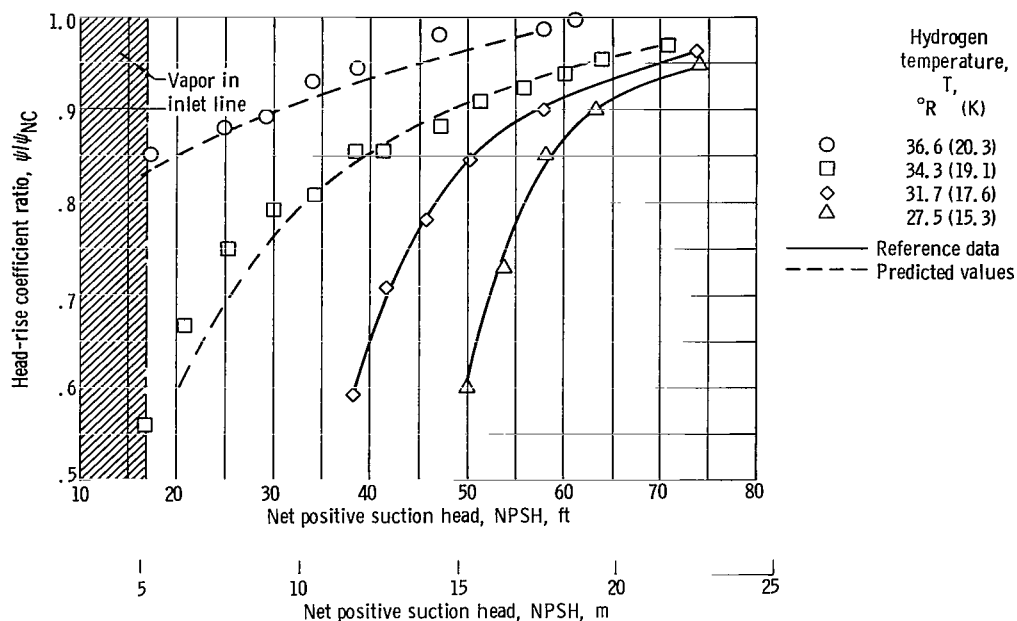


Figure 3. - Comparison of experimental and predicted inducer cavitation performance for an inducer in hydrogen at constant rotational speed of 20 000 rpm and flow coefficient of 0.074.

The data of table I also show that the values of Δh_v increase with decreasing values of the head coefficient ratio ψ/ψ_{NC} . A decrease in the value of ψ/ψ_{NC} implies an increase in the length of cavity present within the blade passages. The analysis shows that Δh_v should increase with cavity length ΔX under otherwise fixed conditions (see eq. (11)). Thus, the trend noted in table I is expected.

At a relatively low value of NPSH, depending on the pump design and mode of operation, a condition can be reached where the static pressure in the inlet line becomes equal to the vapor pressure of the entering liquid. As a result, vapor forms in the inlet line,

TABLE I. - INDUCER CAVITY-PRESSURE

DEPRESSION VALUES

[Rotative speed, 20 000 rpm; flow coefficient, 0.074.]

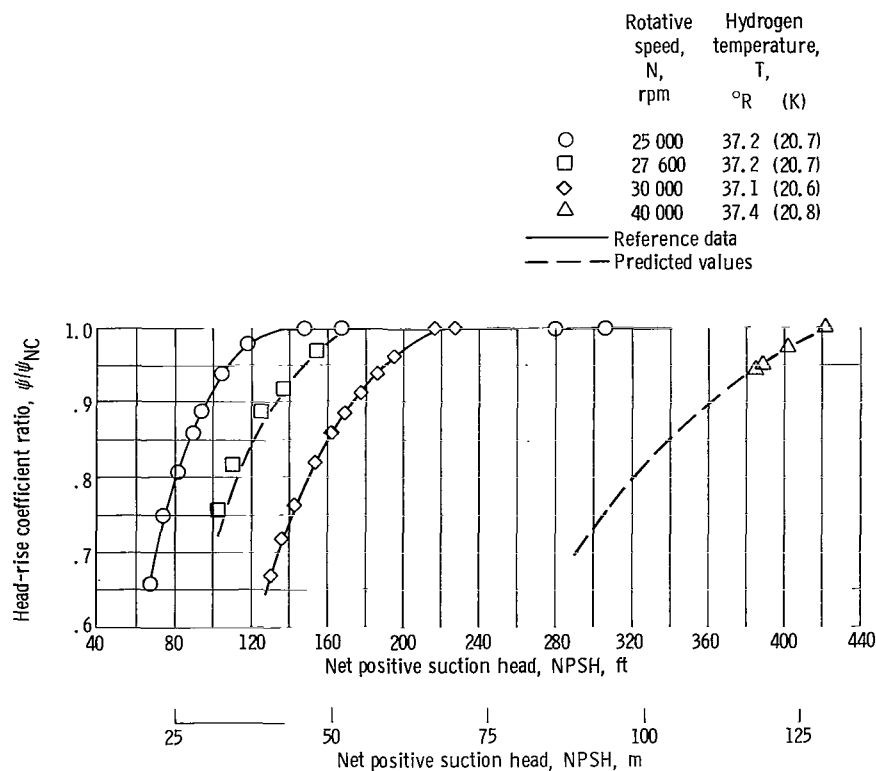
Head-rise coefficient ratio, ψ/ψ_{NC}	Hydrogen temperature, T, °R (K)			
	27.5 (15.3)	31.7 (17.6)	34.3 (19.1)	36.6 (20.3)
	Cavity-pressure depression, Δh_v , ft of liquid (m of liquid)			
0.9	2.0 (0.6)	8.1 (2.5)	17.3 (5.3)	35.0 (10.7)
.8	2.2 (0.7)	11.5 (3.5)	24.0 (7.3)	-----

and any further reductions in NPSH produce increasing amounts of vapor that are ingested by the pump. For the inducer performance data of figure 3, this condition of boiling in the inlet line occurred at an NPSH of about 17 feet (5.2 m). The data for 36.6° R (20.3 K) show that the test inducer was capable of pumping boiling hydrogen while maintaining about 85 percent of the noncavitating head-rise coefficient.

With vapor present in the inlet line, the requirement of flow similarity with respect to reference test conditions is, in general, not met; and thus the present method is not applicable to this mode of operation. The subject of two-phase flow in the inlet line and its effect on inducer cavitation performance in hydrogen is discussed in references 19 and 20.

Pump Cavitation Performance

Impeller A. - Cavitation performance for the 2.67-inch- (6.78-cm-) inlet diameter centrifugal impeller operated in hydrogen at a near-constant temperature of 37.2° R



(a) Flow coefficient, 0.225.

Figure 4. - Comparison of experimental and predicted cavitation performance for impeller A in liquid hydrogen.

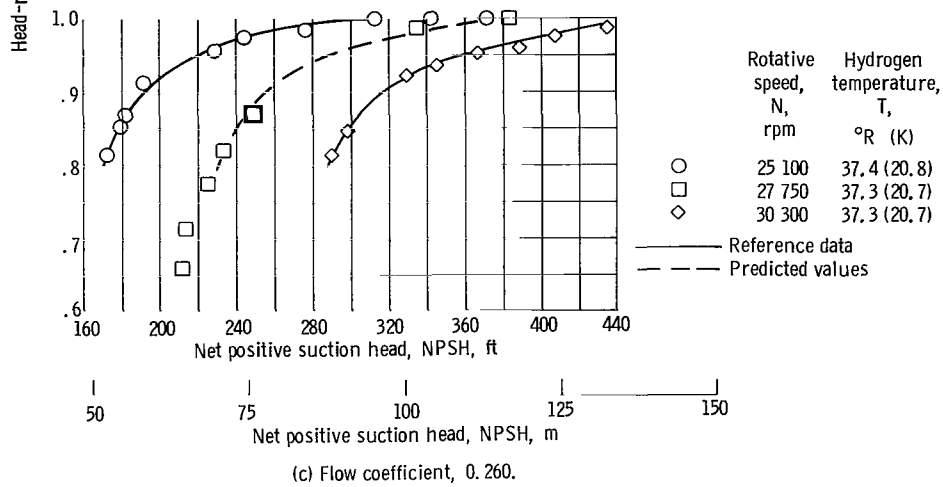
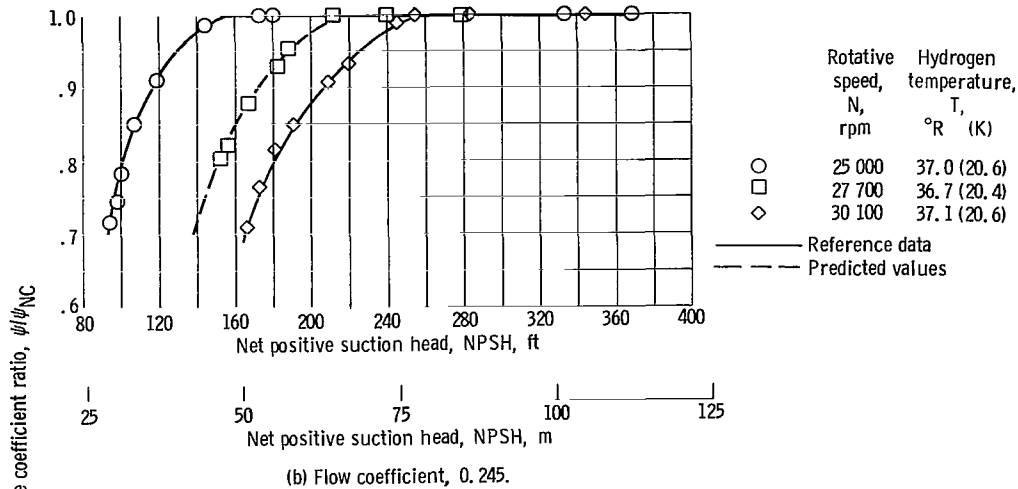


Figure 4. - Concluded.

(20.7 K) is presented in figure 4 for speeds from 25 000 to 40 000 rpm and flow coefficients of 0.225, 0.245, and 0.260. The predicted cavitation performance curves (dashed lines) are all in excellent agreement with the experimental data.

The values of Δh_v realized for this impeller (from data of fig. 4) are listed in table II for a head-rise coefficient ratio of 0.9. Thermodynamic effects of cavitation increased significantly with increasing pump rotative speed. At a flow coefficient of 0.245, the Δh_v value for $N = 27\,700$ rpm is lower than the Δh_v value for $N = 25\,000$ rpm. This apparent lower value of Δh_v is the result of the lower test liquid temperature for this particular set of performance data (see fig. 4(b)).

The thermodynamic effects of cavitation also varied considerably with changes in flow coefficient (table II). This trend was also observed in reference 9. The results of

TABLE II. - IMPELLER A CAVITY-PRESSURE
DEPRESSION VALUES

[Nominal hydrogen temperature, 37.2° R (20.7 K);
head-rise coefficient ratio, 0.9.]

Flow coefficient, ϕ	Nominal rotative speed, N, rpm			
	25 000	27 700	30 000	40 000
	Cavity-pressure depression, Δh_v , ft of liquid (m of liquid)			
0.225	98 (29.9)	103 (31.4)	106 (32.3)	133 (40.5)
.245	112 (34.1)	111 (33.8)	127 (38.7)	-----
.260	110 (33.5)	114 (34.8)	122 (37.2)	-----

reference 21 indicate that the magnitude of thermodynamic effects of cavitation is a function of the noncavitating wall pressure distribution. Since changes in flow coefficient affect the pressure distribution on the pump blades, this variation in thermodynamic effects with flow coefficient is to be expected.

Because of the rapid change in the physical properties of hydrogen with temperature, the seemingly small variation in temperature of about 0.3° R (0.2 K) between the various performance curves, as in figure 4(a), must be accounted for if reasonably accurate predictions are to be realized. For N = 40 000 rpm and $\psi/\psi_{NC} = 0.9$, for example, the predicted value of NPSH would have been 380 feet (115.8 m) of hydrogen instead of 361 feet (110.0 m) if the temperature for all the performance curves of figure 4(a) had been assumed to be constant at 37.1° R (20.6 K).

Impeller B. - Experimental and predicted results for the 3.86-inch- (9.80-cm-) inlet diameter impeller operated in hydrogen at nearly constant temperature for three rotational speeds are presented in figure 5. The predicted cavitation performance (dashed line) is in good agreement with the experimental data. As with pump impeller A, the thermodynamic effects of cavitation increase significantly with pump speed, as can be noted by the Δh_v values listed in table III. However, for a comparable hydrogen temperature, the magnitudes of the thermodynamic effects for this impeller exceed the largest value noted for either the inducer or impeller A. The reason for these large changes in thermodynamic effects of cavitation with rotor design is not known at present.

An examination of the Δh_v values of tables I to III show conclusively that thermodynamic effects of cavitation in liquid hydrogen are substantial. These effects depend on liquid temperature, rotor type and geometric design, rotative speed, flow coefficient ϕ , and, to some extent, head-rise coefficient ratio ψ/ψ_{NC} .

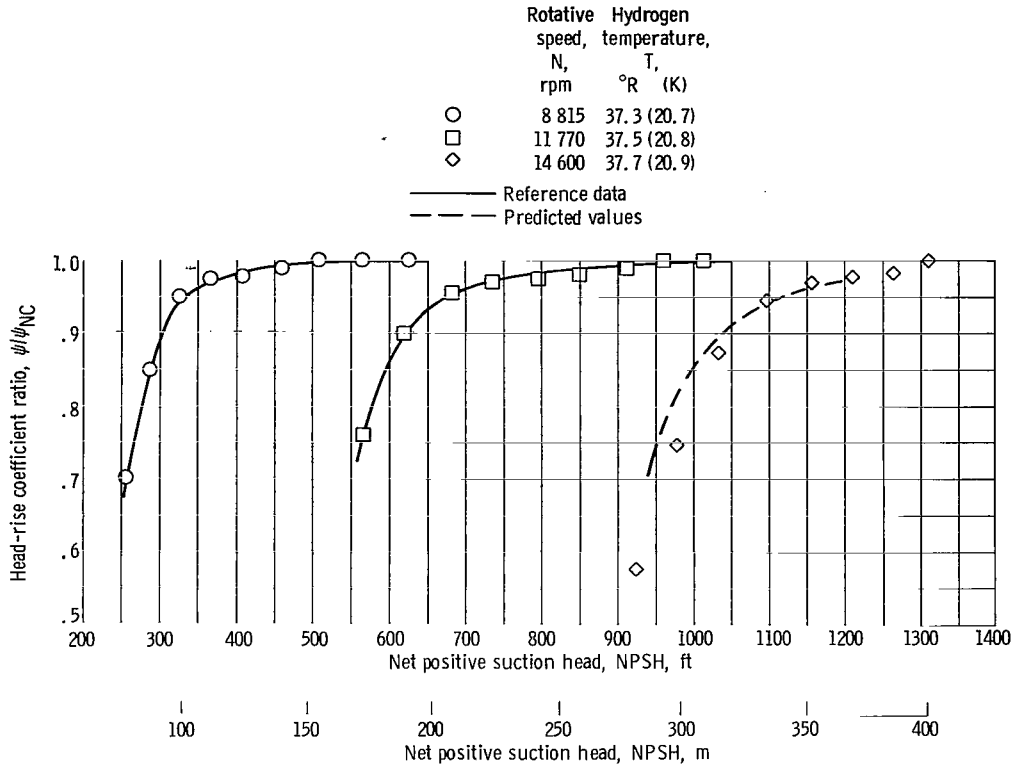


Figure 5. - Comparison of experimental and predicted cavitation performance for impeller B in liquid hydrogen. Flow coefficient, 0.44.

TABLE III. - IMPELLER B CAVITY-PRESSURE

DEPRESSION VALUES

[Flow coefficient, 0.44; head-rise coefficient ratio, 0.9]

Rotative speed, N, rpm	Hydrogen temperature, T		Cavity-pressure depression, Δh_v	
	°R	K		
			ft of liquid	m of liquid
8 815	37.3	20.7	141	43.0
11 770	37.5	20.8	171	52.1
14 600	37.7	20.9	199	60.7

Commercial pumps. - The prediction method was also used to predict the cavitation performance for several small commercial pumps operated in a variety of liquids at various temperatures. The measured and predicted NPSH requirements for three single-stage centrifugal units pumping water, methyl alcohol, butane, and Freon-11 are compared in table IV. The NPSH values listed are taken from references 1 and 2. All values are for a head-rise coefficient ratio ψ/ψ_{NC} of 0.97, a pump speed of about 3550 rpm, and the operating point of best efficiency. The two reference test values of

TABLE IV. - COMPARISONS OF MEASURED AND PREDICTED
PUMP CAVITATION PERFORMANCE

[Nominal rotative speed, 3550 rpm; head-rise coefficient ratio, 0.97]

Pump	Liquid	Temperature, T		Net positive suction head, NPSH			
		°R	K	ft		m	
				Measured (±0.5 ft)	Predicted	Measured (±0.2 m)	Predicted
I (ref. 2)	Water	534	297	^a 17.5	----	^a 5.3	---
		600	333	17.5	17.5	5.3	5.3
		670	372	17.5	17.4	5.3	5.3
		710	394	^a 17.0	----	^a 5.2	---
		735	408	16.0	16.5	4.9	5.0
		756	420	13.3	15.6	4.1	4.8
	Methyl alcohol	560	311	17.5	17.4	5.3	5.3
		611	339	16.7	16.8	5.1	5.1
		641	356	15.5	15.3	4.7	4.7
		663	368	13.5	13.3	4.1	4.1
II (ref. 1)	Water	530	294	12.3	11.8	3.7	3.6
		710	394	^a 11.0	----	^a 3.4	---
		760	422	8.6	8.7	2.6	2.7
	Butane	495	275	9.8	10.2	3.0	3.1
		515	286	^a 8.8	----	^a 2.7	---
		540	300	5.1	5.6	1.6	1.7
		550	306	3.5	3.4	1.1	1.0
	Freon-11	545	303	10.2	10.5	3.1	3.2
		580	322	8.4	8.1	2.6	2.5
	III (ref. 1)	Water	530	294	^a 12.0	----	^a 3.7
750			417	^a 9.5	----	^a 2.9	---
785			436	6.0	6.0	1.8	1.8
870			483	^b 2.0	0	0.6	0

^aReference test data.

^bEstimated accuracy of 2.0 ft (0.6 m).

NPSH listed for each pump (noted by (a)) were arbitrarily chosen to determine reference values of vapor- to liquid-volume ratio $(\nu_v/\nu_l)_{\text{ref}}$ and subsequently $(\Delta h_v)_{\text{ref}}$ for use in the prediction method. The predicted results are in excellent agreement with the experimental data. In fact, except for the 756° R (420 K) water data for pump I, the predicted values are all within the experimental accuracy of measured NPSH values.

For pump III operated in 870° R (483 K) water, the predicted NPSH value is zero, which implies that this pump should have been capable of satisfactory operation at an NPSH value sufficiently low to cause vapor to form in the inlet line. Reference 2 states that there were indeed indications of flashing in the inlet line at rated flow.

As a consequence, the listed NPSH value of 2.0 feet (0.6 m) of water was actually determined by extrapolation of performance data obtained at less-than-design flow rates. This set of data, as well as the hydrogen data of figure 3, illustrates that it is possible to pump boiling liquids satisfactorily if the fluid being pumped has sufficiently high thermodynamic effects of cavitation.

CONCLUDING REMARKS

The method for predicting the cavitation performance of pumps presented herein provided consistently good agreement between predicted and experimental results for several different pumps operated in liquids having widely diverse physical properties. Use of the method requires that two sets of test data, at least one of which provides measurable thermodynamic effects, be available for the pump and operating conditions of interest. However, the test data need not necessarily be for the same liquid, liquid temperature, or pump rotative speed. From these reference tests, accurate predictions of cavitation performance for a given pump can be made for any liquid, liquid temperature, and pump rotative speed provided that a condition of flow similarity is maintained.

The method also has useful application in the generalization of experimental data obtained with liquids that exhibit substantial thermodynamic effects of cavitation. Pump studies involving a particular liquid, for example, need not be conducted at precise values of liquid temperature or rotative speed since, by use of the present method, the data can be normalized or adjusted to any convenient liquid temperature or pump speed. Use of the prediction method may provide substantial reductions in the cost and development time required for new pump designs, particularly for those used in the aerospace field. It should be possible to conduct development testing at reduced speed using convenient or easy-to-handle liquids that exhibit thermodynamic effects of cavitation, such as Freon or high-temperature water; from these tests, the cavitation performance for the liquid and operating condition of interest may be predicted.

Although additional studies are required to prove the validity of the method to size effects for geometrically similar pumps, additional substantial savings are possible if the method can be used to accurately predict the cavitation performance for a full-scale pump from test results obtained for smaller prototypes.

Lewis Research Center,
National Aeronautics and Space Administration,
Cleveland, Ohio, March 27, 1969,
128-31-32-12-22.

APPENDIX A

SYMBOLS

C_l	specific heat of liquid, Btu/(lbm)(^o R); J/(kg)(K)
D	characteristic body dimension, in.; cm
g	local acceleration due to gravity, 32.163 ft/sec ² ; 9.80 m/sec ²
g_c	dimensional constant, 32.174 (ft)(lbm)/(sec ²)(lbf); 1.0 (m)(kg)/(sec ²)(N)
ΔH	pump or inducer head rise, ft of liquid; m of liquid
h_c	pressure in cavitated region, ft of liquid abs; m of liquid abs
h_0	free-stream or pump inlet static pressure, ft of liquid abs; m of liquid abs
h_v	vapor pressure corresponding to free-stream temperature, ft of liquid abs; m of liquid abs
Δh_v	decrease in vapor pressure due to vaporization, ft of liquid; m of liquid
J	mechanical equivalent of heat, 778 (ft)(lbf)/Btu
K	developed cavitation parameter based on free-stream vapor pressure, $(h_0 - h_v)/(V_0^2/2g)$
$K_{c,min}$	developed cavitation parameter based on minimum cavity pressure, $(h_0 - h_{c,min})/(V_0^2/2g)$
k	thermal conductivity of saturated liquid, (Btu)(ft)/(hr)(ft ²)(^o R); J/(m)(sec)(K)
L	latent heat of vaporization, Btu/lbm; J/kg
N	rotative speed, rpm
T	free-stream liquid temperature, ^o R; K
ΔT	decrease in local equilibrium temperature due to vaporization, ^o R; K
U_T	blade tip velocity, ft/sec; m/sec
V_0	free-stream velocity, ft/sec; m/sec
V_1	mean axial inlet velocity, ft/sec; m/sec
\mathcal{V}_l	volume of saturated liquid, cu ft; cu m
\mathcal{V}_v	volume of saturated vapor, cu ft; cu m
ΔX	length of cavitated region, in.; cm
α	thermal diffusivity, $k/\rho_l C_l$, ft ² /hr; m ² /hr

ν_l	specific volume of saturated liquid, cu ft/lbm; cu m/kg
ν_v	specific volume of saturated vapor, cu ft/lbm; cu m/kg
ρ_l	saturated liquid density, lbm/cu ft; kg/cu m
ρ_v	saturated vapor density, lbm/cu ft; kg/cu m
ϕ	flow coefficient, V_1/U_T
ψ	head-rise coefficient, $\Delta H/U_T^2$

Subscripts:

min	minimum
NC	noncavitating
pred	predicted value
ref	reference value obtained from experimental tests

APPENDIX B

NUMERICAL EXAMPLES

Example 1 - Prediction Based on Test Data Obtained for a Given Liquid at Various Temperatures

Cavitation performance curves are available for an inducer operated at a constant flow coefficient and rotative speed in liquid hydrogen at 27.5° and 31.7° R (15.3 and 17.6 K); see figure 3.

To be determined is the inducer NPSH required for 36.6° R (20.3 K) liquid hydrogen at a head-rise coefficient ratio of 0.9 for the same operating conditions.

From the analysis presented earlier,

$$\frac{\text{NPSH}_{\text{ref}} + (\Delta h_v)_{\text{ref}}}{\text{NPSH} + \Delta h_v} = \left(\frac{N_{\text{ref}}}{N} \right)^2 \quad (\text{B1})$$

and

$$\left(\frac{\gamma_v}{\gamma_l} \right)_{\text{pred}} = \left(\frac{\gamma_v}{\gamma_l} \right)_{\text{ref}} \left(\frac{N}{N_{\text{ref}}} \right)^{0.8} \left(\frac{\alpha_{\text{ref}}}{\alpha} \right)^{1.0} \quad (\text{B2})$$

With 27.5° R (15.3 K) hydrogen data arbitrarily chosen for reference conditions, the values of NPSH for a head-rise coefficient ratio of 0.9 (from fig. 3) are

$$\text{NPSH}_{\text{ref}} = 63.5 \text{ ft (19.4 m)} \quad \text{for } T_{\text{ref}} = 27.5^\circ \text{ R (15.3 K)}$$

$$\text{NPSH} = 57.4 \text{ ft (17.5 m)} \quad \text{for } T = 31.7^\circ \text{ R (17.6 K)}$$

For this example, $N_{\text{ref}} = N$; $\alpha_{\text{ref}} = 7.71 \times 10^{-3}$ square feet per hour ($7.16 \times 10^{-4} \text{ m}^2/\text{hr}$); $\alpha = 7.23 \times 10^{-3}$ square feet per hour ($6.71 \times 10^{-4} \text{ m}^2/\text{hr}$). Substitution of these values into equations (B1) and (B2) yields

$$\Delta h_v - (\Delta h_v)_{\text{ref}} = 6.1 \text{ ft (1.9 m)}$$

and

$$\left(\frac{\gamma_v}{\gamma_l}\right) = 1.07 \left(\frac{\gamma_v}{\gamma_l}\right)_{\text{ref}}$$

An iterative solution of these two expressions using the curves of figure 1(a) results in the following:

$$\left(\frac{\gamma_v}{\gamma_l}\right)_{\text{ref}} = 0.25$$

and

$$(\Delta h_v)_{\text{ref}} = 2.0 \text{ ft (0.6 m)}$$

For hydrogen at 36.6° R (20.3 K), $\alpha = 6.69 \times 10^{-3}$ square feet per hour ($6.22 \times 10^{-4} \text{ m}^2/\text{hr}$). With the use of this value for α and the foregoing reference value for $(\gamma_v/\gamma_l)_{\text{ref}}$ in equation (B2), the predicted $(\gamma_v/\gamma_l)_{\text{pred}}$ for 36.6° R (20.3 K) hydrogen is

$$\left(\frac{\gamma_v}{\gamma_l}\right)_{\text{pred}} = 0.25 (1.0) \left(\frac{7.7 \times 10^{-3}}{6.69 \times 10^{-3}}\right) = 0.29$$

From figure 1(a), the corresponding value for Δh_v is 35.0 feet (10.7 m). The predicted value of required NPSH for 36.6° R (20.3 K) hydrogen is obtained by substitution of the reference values and Δh_v into equation (B1); thus,

$$\text{NPSH} = 63.5 + 2.0 - 35.0 = 30.5 \text{ ft (9.3 m)}$$

The corresponding measured value of NPSH is about 30.0 feet (9.1 m).

Example 2 - Prediction Based on Test Data Obtained with a Given Liquid at Different Temperatures and Pump Rotative Speeds

Cavitation performance curves are available for a pump handling 37.2° R (20.7 K) hydrogen at 25 000 rpm and 37.1° R (20.6 K) hydrogen at 30 000 rpm at a constant flow coefficient of 0.225 (see fig. 4(a)).

To be determined is the pump NPSH required with 37.4^o R (20.8 K) hydrogen for a head-rise coefficient ratio of 0.95, a pump speed of 40 000 rpm, and the same flow coefficient.

With the data for 25 000 rpm arbitrarily taken as reference conditions, the NPSH values for a head-rise coefficient ratio of 0.95 (from fig. 4(a)) are

$$\text{NPSH}_{\text{ref}} = 107.5 \text{ ft (32.8 m)} \quad \text{for } 25\,000 \text{ rpm} = N_{\text{ref}}$$

$$\text{NPSH} = 190.0 \text{ ft (57.9 m)} \quad \text{for } 30\,000 \text{ rpm} = N$$

Substitution of these values in equations (B1) and (B2) yields

$$(\Delta h_v)_{\text{ref}} - 0.695 \Delta h_v = 24.5 \text{ ft (7.5 m)}$$

$$\left(\frac{\gamma_v}{\gamma_l}\right) = 1.16 \left(\frac{\gamma_v}{\gamma_l}\right)_{\text{ref}}$$

An iterative solution of the two preceding expressions using the curves of figure 1(a) results in the following reference values: (Note: for this example, changes in α (eq. (B2)) are negligible; but effects of small changes in hydrogen temperature are accounted for in the use of curves of fig. 1.)

$$\left(\frac{\gamma_v}{\gamma_l}\right)_{\text{ref}} = 0.80; \quad (\Delta h_v)_{\text{ref}} = 98.0 \text{ ft (29.9 m)} \quad \text{at } 25\,000 \text{ rpm}$$

Substituting $(\gamma_v/\gamma_l)_{\text{ref}}$ into equation (B2) gives the value of $(\gamma_v/\gamma_l)_{\text{pred}}$ for 40 000 rpm

$$\left(\frac{\gamma_v}{\gamma_l}\right)_{\text{pred}} = 0.8 \left(\frac{40\,000}{25\,000}\right)^{0.8} = 1.17 \quad \text{where } \alpha = \alpha_{\text{ref}}$$

From figure 1(a), the corresponding value of Δh_v at 37.4^o R (20.8 K) is 134.0 feet (40.8 m). Substituting for Δh_v and N in equation (B1) and solving for NPSH yields

$$(\text{NPSH})_{\text{pred}} = \frac{107.5 + 98.0}{\left(\frac{25\,000}{40\,000}\right)^2} - 134.0 = 392.1 \text{ ft (119.5 m)}$$

The corresponding measured value from figure 4(a) is about 387 feet (118.0 m).

Example 3 - Prediction Based on Test Data Obtained Using Different Liquids

The NPSH requirements are given for pump II (table IV) handling 710° R (394 K) water and 515° R (286 K) butane at fixed operating conditions (3550 rpm and $\psi/\psi_{\text{NC}} = 0.97$).

To be determined is the pump NPSH required for 550° R (306 K) butane under the same operating conditions.

With the water data arbitrarily chosen for reference, the NPSH values (from table IV) are

$$\text{NPSH}_{\text{ref}} = 11.0 \text{ ft (3.4 m)} \quad \text{for } 710^{\circ} \text{ R (394 K) water}$$

$$\text{NPSH} = 8.8 \text{ ft (2.7 m)} \quad \text{for } 515^{\circ} \text{ R (286 K) butane}$$

Values of liquid thermal diffusivity α are 6.60×10^{-3} square feet per hour (6.13×10^{-4} m²/hr) for 710° R (395 K) water and 4.02×10^{-3} square feet per hour (3.73×10^{-4} m²/hr) for 515° R (286 K) butane. Substituting the foregoing values of NPSH and α into equations (B1) and (B2) yields

$$\Delta h_v - (\Delta h_v)_{\text{ref}} = 2.2 \text{ ft (0.7 m)}$$

$$\left(\frac{\gamma_v}{\gamma_l}\right) = 1.64 \left(\frac{\gamma_v}{\gamma_l}\right)_{\text{ref}}$$

An iterative solution of the above relations using the curves of figure 1(b) gives

$$\left(\frac{\gamma_v}{\gamma_l}\right)_{\text{ref}} = 0.49; \quad (\Delta h_v)_{\text{ref}} = 0.7 \text{ ft (0.2 m)}$$

Substituting $(\gamma_v/\gamma_l)_{\text{ref}}$ into equation (B2) yields the predicted value of (γ_v/γ_l) for 550°R (306 K) butane

$$\left(\frac{\gamma_v}{\gamma_l}\right)_{\text{pred}} = 0.49 (1.0) \left(\frac{6.60 \times 10^{-3}}{4.02 \times 10^{-3}}\right) = 0.80$$

for butane, $\alpha_{550^\circ \text{R}} = \alpha_{515^\circ \text{R}}$. From figure 1(b), the corresponding value of Δh_v is 8.3 feet (2.5 m). Thus, from equation (B1), the predicted NPSH for pump II (table IV) pumping 550°R (306 K) butane at 3550 rpm and a head-rise coefficient ratio of 0.97 is

$$\text{NPSH}_{\text{pred}} = 11.0 + 0.7 - 8.3 = 3.4 \text{ ft (1.0 m)}$$

From table IV, the corresponding measured NPSH is 3.5 feet (1.1 m).

REFERENCES

1. Salemann, Victor: Cavitation and NPSH Requirements of Various Liquids. *J. Basic Eng.*, vol. 81, no. 2, June 1959, pp. 167-180.
2. Spraker, W. A.: The Effects of Fluid Properties on Cavitation in Centrifugal Pumps. *J. Eng. Power*, vol. 87, no. 3, July 1965, pp. 309-318.
3. Wilcox, Ward W.; Meng, Phillip R.; and Davis, Roger L.: Performance of an Inducer-Impeller Combination at or Near Boiling Conditions for Liquid Hydrogen. *Advances in Cryogenic Engineering*. Vol. 8, K. D. Timmerhaus, ed., Plenum Press, Inc., 1963, pp. 446-455.
4. Jacobs, Robert B.: Prediction of Symptoms of Cavitation. *J. Res. Natl. Bur. Std.*, sec. C, vol. 65, no. 3, July-Sept. 1961, pp. 147-156.
5. Stahl, H. A.; and Stepanoff, A. J.: Thermodynamic Aspects of Cavitation in Centrifugal Pumps. *Trans. ASME*, vol. 78, no. 8, Nov. 1956, pp. 1691-1963.
6. Stepanoff, A. J.: Cavitation in Centrifugal Pumps with Liquids Other Than Water. *J. Eng. Power*, vol. 83, no. 1, Jan. 1961, pp. 79-90.
7. Stepanoff, A. J.: Cavitation Properties of Liquids. *J. Eng. Power*, vol. 86, no. 2, Apr. 1964, pp. 195-200.
8. Ball, Calvin L.; Meng, Phillip R.; and Reid, Lonnie: Cavitation Performance of 84° Helical Pump Inducer Operated in 37° and 42° R Liquid Hydrogen. NASA TM X-1360, 1967.
9. Meng, Phillip R.: Change in Inducer Net Positive Suction Head Requirement with Flow Coefficient in Low Temperature Hydrogen (27.9° to 36.6° R). NASA TN D-4423, 1968.
10. Gelder, Thomas F.; Ruggeri, Robert S.; and Moore, Royce D.: Cavitation Similarity Considerations Based on Measured Pressure and Temperature Depressions in Cavitated Regions of Freon-114. NASA TN D-3509, 1966.
11. Moore, Royce D.; and Ruggeri, Robert S.: Venturi Scaling Studies on Thermodynamic Effects of Developed Cavitation of Freon-114. NASA TN D-4387, 1968.
12. Ruggeri, Robert S.; and Gelder, Thomas F.: Cavitation and Effective Liquid Tension of Nitrogen in a Tunnel Venturi. NASA TN D-2088, 1964.
13. Pinkel, I. Irving; Hartmann, Melvin J.; Hauser, Cavour H.; Miller, Max J.; Ruggeri, Robert S.; and Soltis, Richard F.: Pump Technology. Selected Technology for the Petroleum Industry. NASA SP-5053, 1966, pp. 81-101.

14. Ruggeri, Robert S.; Moore, Royce D.; and Gelder, Thomas F.: Method for Predicting Pump Cavitation Performance. Paper presented at the ICRPG Ninth Liquid Propulsion Symposium, St. Louis, Oct. 25-27, 1967.
15. Hord, Jesse; Edmonds, Dean K.; and Millhiser, David R.: Thermodynamic Depressions Within Cavities and Cavitation Inception in Liquid Hydrogen and Liquid Nitrogen. Rep. 9705, National Bureau of Standards (NASA CR-72286), Mar. 1968.
16. Moore, Royce D.; and Ruggeri, Robert S.: Prediction of Thermodynamic Effects of Developed Cavitation Based on Liquid-Hydrogen and Freon-114 Data in Scaled Venturi. NASA TN D-4899, 1968.
17. Urasek, Donald C.: Investigation of Flow Range and Stability of Three Inducer-Impeller Pump Combinations Operating in Liquid Hydrogen. NASA TM X-1727, 1969.
18. Miller, Max J.; and Soltis, Richard F.: Detailed Performance of a Radial-Bladed Centrifugal Pump Impeller in Water. NASA TN D-4613, 1968.
19. Meng, Phillip R.; and Connelly, Robert E.: Investigation of Effects of Simulated Nuclear Radiation Heating on Inducer Performance in Liquid Hydrogen. NASA TM X-1359, 1967.
20. Urasek, Donald C.; Meng, Phillip R.; and Connelly, Robert E.: Cavitation Performance of 80.6° Helical Inducer in Liquid Hydrogen. NASA TN D-5258, 1969.
21. Moore, Royce D.; Ruggeri, Robert S.; and Gelder, Thomas F.: Effects of Wall Pressure Distribution and Liquid Temperature on Incipient Cavitation of Freon-114 and Water in Venturi Flow. NASA TN D-4340, 1968.

